

# Terahertz sideband-tuned quantum cascade laser radiation

Andriy A. Danylov<sup>1\*</sup>, Jerry Waldman<sup>1</sup>, Thomas M. Goyette<sup>1</sup>, Andrew J. Gatesman<sup>1</sup>, Robert H. Giles<sup>1</sup>, Jin Li<sup>2</sup>, William D. Goodhue<sup>2</sup>, Kurt J. Linden<sup>3</sup>, and William E. Nixon<sup>4</sup>

<sup>1</sup> Submillimeter-Wave Technology Laboratory, Dept. of Physics and Applied Physics,  
University of Massachusetts Lowell,  
Lowell, Massachusetts, 01854, USA

<sup>2</sup> Photonics Center, Dept. of Physics and Applied Physics, University of Massachusetts Lowell,  
Lowell, Massachusetts, 01854, USA

<sup>3</sup> Spire Corporation, Bedford, Massachusetts, 01730, USA

<sup>4</sup> U.S. Army National Ground Intelligence Center, Charlottesville, Virginia 22911, USA

\*Corresponding author: [Andriy.Danylov@student.uml.edu](mailto:Andriy.Danylov@student.uml.edu)

**Abstract:** A compact, tunable, narrowband terahertz source was demonstrated by mixing a single longitudinal mode 2.408 THz, free running quantum cascade laser with a 2-20 GHz microwave sweeper in a conventional corner-cube-mounted Schottky diode. The sideband spectra were characterized with a Fourier transform spectrometer, and the radiation was tuned through several D<sub>2</sub>O rotational transitions to estimate the longer term ( $t \geq$  several sec) bandwidth of the source. A spectral resolution of 2 MHz in CW regime was observed.

©2008 Optical Society of America

**OCIS codes:** (140.5965) Semiconductor lasers, quantum cascade; (190.2620) Harmonic generation and mixing; (300.1030) Absorption; (300.3700) Linewidth; (300.6270) Spectroscopy, far infrared.

---

## References and links

1. B. S. Williams, S. Kumar, Q. Hu, and J. L. Reno, "High-power terahertz quantum-cascade lasers," *Electron. Lett.* **42**, 89 (2006).
2. M. S. Vitiello, G. Scamarcio, V. Spagnolo, S. S. Dhillon, and C. Sirtori, "Terahertz quantum cascade lasers with large wall-plug efficiency," *Appl. Phys. Lett.* **90**, 191115 (2007).
3. C. Walther, G. Scalari, J. Faist, H. Beere, & D. Ritchie, "Low frequency terahertz quantum cascade laser operating from 1.6 to 1.8 THz," *Appl. Phys. Lett.* **89**, 231121 (2006).
4. A. Barkan, *et al.*, "Linewidth and tuning characteristics of terahertz quantum cascade lasers," *Opt. Lett.* **29**, 575 (2004).
5. S. Barbieri, *et.al.*, "Heterodyne mixing of two far-infrared quantum cascade lasers by use of a point-contact Schottky diode," *Opt. Lett.* **29**, 1632 (2004).
6. A. Baryshev, *et.al.*, "Phase locking and spectral linewidth of a two-mode terahertz quantum cascade laser," *Appl. Phys. Lett.* **89**, 031115 (2006).
7. A. L. Betz, R. T. Boreiko, B. S. Williams, S. Kumar, Q. Hu, and J. L. Reno, "Frequency and phase-lock control of a 3 THz quantum cascade laser," *Opt. Lett.* **30**, 1837 (2005).
8. K. M. Evenson, D. A. Jennings, and F. R. Peterson, "Tunable far-infrared spectroscopy," *Appl. Phys. Lett.* **44**, 576-578 (1984).
9. D. D. Bicanic, B. F. J. Zuidberg, and A. Dymanus, "Generation of continuously tunable laser sidebands in the submillimeter region," *Appl. Phys. Lett.* **32**, 367-369 (1978).
10. W. A. M. Blumberg, H. R. Fetterman, D. D. Peck, and P. F. Goldsmith, "Tunable submillimeter sources applied to the excited state rotational spectroscopy and kinetics of CH<sub>3</sub>F," *Appl. Phys. Lett.* **35**, 582-585 (1979).
11. T. D. Varburg and K. M. Evenson, "Laser spectroscopy of carbon monoxide: a frequency reference for the far infrared," *IEEE Trans. Inst. and Meas.* **42**, 412 (1993).
12. R. Gendriesch, F. Lewen, G. Winnewisser, and J. Han, "Precision Broadband Spectroscopy near 2 THz: Frequency-Stabilized Laser Sideband Spectrometer with Backward-Wave Oscillators," *J. Mol. Spectrosc.* **203**, 205 (2000).
13. B. J. Drouin, F. W. Maiwald, and J. C. Pearson, "Application of cascaded frequency multiplication to molecular spectroscopy," *Rev. Sci. Instrum.* **76**, 093113 (2005).
14. [www.virginiadiodes.com](http://www.virginiadiodes.com).

<b>Report Documentation Page</b>			Form Approved OMB No. 0704-0188	
<p>Public reporting burden for the collection of information is estimated to average 1 hour per response, including the time for reviewing instructions, searching existing data sources, gathering and maintaining the data needed, and completing and reviewing the collection of information. Send comments regarding this burden estimate or any other aspect of this collection of information, including suggestions for reducing this burden, to Washington Headquarters Services, Directorate for Information Operations and Reports, 1215 Jefferson Davis Highway, Suite 1204, Arlington VA 22202-4302. Respondents should be aware that notwithstanding any other provision of law, no person shall be subject to a penalty for failing to comply with a collection of information if it does not display a currently valid OMB control number.</p>				
1. REPORT DATE <b>27 MAR 2008</b>	2. REPORT TYPE	3. DATES COVERED <b>00-00-2008 to 00-00-2008</b>		
4. TITLE AND SUBTITLE <b>Terahertz sideband-tuned quantum cascade laser radiation</b>			5a. CONTRACT NUMBER	
			5b. GRANT NUMBER	
			5c. PROGRAM ELEMENT NUMBER	
6. AUTHOR(S)			5d. PROJECT NUMBER	
			5e. TASK NUMBER	
			5f. WORK UNIT NUMBER	
7. PERFORMING ORGANIZATION NAME(S) AND ADDRESS(ES) <b>University of Massachusetts Lowell,Submillimeter-Wave Technology Laboratory,Dept. of Physics and Applied Physics,Lowell,MA,01854</b>			8. PERFORMING ORGANIZATION REPORT NUMBER	
9. SPONSORING/MONITORING AGENCY NAME(S) AND ADDRESS(ES)			10. SPONSOR/MONITOR'S ACRONYM(S)	
			11. SPONSOR/MONITOR'S REPORT NUMBER(S)	
12. DISTRIBUTION/AVAILABILITY STATEMENT <b>Approved for public release; distribution unlimited</b>				
13. SUPPLEMENTARY NOTES				
14. ABSTRACT <b>A compact, tunable, narrowband terahertz source was demonstrated by mixing a single longitudinal mode 2.408 THz, free running quantum cascade laser with a 2-20 GHz microwave sweeper in a conventional corner-cube-mounted Schottky diode. The sideband spectra were characterized with a Fourier transform spectrometer, and the radiation was tuned through several D<sub>2</sub>O rotational transitions to estimate the longer term (t &gt; several sec) bandwidth of the source. A spectral resolution of 2 MHz in CW regime was observed.</b>				
15. SUBJECT TERMS				
16. SECURITY CLASSIFICATION OF:			17. LIMITATION OF ABSTRACT <b>Same as Report (SAR)</b>	18. NUMBER OF PAGES <b>10</b>
a. REPORT <b>unclassified</b>	b. ABSTRACT <b>unclassified</b>	c. THIS PAGE <b>unclassified</b>		

15. E. R. Brown, K. A. McIntosh, K. B. Nichols, and C. L. Dennis, "Photomixing up to 3.8 THz in low-temperature-grown GaAs," *Appl. Phys. Lett.* **66**, 285-287 (1995).
  16. A.S. Pine, R.D. Suenram, E.R. Brown, and K.A. McIntosh, "A Terahertz Photomixing Spectrometer: Application to SO<sub>2</sub>Self Broadening J. Mol. Spectrosc. **175**, 37-47 (1996).
  17. S. M. Duffy, S. Verghese, K. A. McIntosh, A. Jackson, A. C. Gossard, and S. Matsuura, *IEEE Trans. Microwave Theory Tech.* **49**, 1032 (2001).
  18. K. Namjou, S. Cai, E. A. Whittaker, J. Faist, C. Gmachl, F. Capasso, D. L. Sivco, and A.Y. Cho, "Sensitive absorption spectroscopy with a room-temperature distributed-feedback quantum-cascade laser," *Opt. Lett.* **23**, 219 (1998).
  19. S. Barbieri, J. Alton, H. E. Beere, J. Fowler, E. H. Linfield, and D. A. Ritchie, *Appl. Phys. Lett.*, **85**, 1674 2004.
  20. J. Li, X. Qian, W. Liu, S. R. Vangala, W. D. Goodhue, A. A. Danylov, J. Waldman, R. H. Giles, and K. J. Linden, *The 20th Annual Meeting of the IEEE, Lasers and Electro-Optics Society, 2007*. 21-25 Oct. 2007, pgs. 860 – 861.
  21. A. A. Danylov, J. Waldman, T. M. Goyette, A. J. Gatesman, R. H. Giles, K. J. Linden, W. E. Nixon, M. C. Wanke, and J. L. Reno, "Transformation of the multimode terahertz quantum cascade laser beam into a Gaussian, using a hollow dielectric waveguide," *Appl. Opt.* **46**, 5051-5055 (2007).
  22. Thomas Keating Ltd, Billingham, West Sussex, England.
  23. C. H. Townes, A. L. Schawlow, *Microwave Spectroscopy* (Dover Publications, 1975), Chap. 13.
  24. <http://spec.jpl.nasa.gov/ftp/pub/catalog/catform.html>
- 

## 1. Introduction

Terahertz (THz) quantum cascade laser (TQCL) development is progressing rapidly, with demonstrations of higher power [1], improved efficiency [2], and longer wavelength operation [3]. The short term ( $t_s \sim$  milliseconds) and longer term ( $t_l \sim 10$  sec) frequency spectra of a free running, 4.7 THz QCL have been measured [4], with values of  $(\Delta\nu)_s \approx 30\text{kHz}$  and  $(\Delta\nu)_l \approx 20\text{MHz}$ , respectively. The larger value of  $(\Delta\nu)_l$  is attributed to index of refraction changes due to fluctuations in temperature during the sampling interval. Measurement of  $(\Delta\nu)_s$  is more difficult and the results to date [4-6] should be viewed only as an upper limit to the instantaneous laser linewidth.

Active stabilization of a TQCL's frequency has been demonstrated. Betz, et. al. [7], achieved a 65 kHz, 3dB bandwidth by locking a 3.06 THz QCL to an optically pumped gas laser. With further improvements in power and spatial mode quality, it should be possible to lock a TQCL to the harmonic of an ultra-stable microwave source. However, even the 20 MHz resolution of an unlocked TQCL rivals all but the highest resolution THz sources, which require either (1), a pair of stabilized CO<sub>2</sub> lasers [8], or (2), a stable CO<sub>2</sub> pumped far-infrared molecular laser system [9-10]. Combined with a synthesized microwave swept source in a nonlinear mixer, these systems have achieved remarkable spectral resolution, on the order of 10 kHz [11-12], but equipment assembly and maintenance costs limit the availability of such systems. Recently, frequency multiplied solid state (FMSS) chains operating up to 2.65 THz have been demonstrated [13] and such sources are now commercially available up to 1.55 THz [14]. FMSS sources rival the previously mentioned laser-hybrid methods in resolution, but power levels currently fall off rapidly above 1.5 THz. Photomixer techniques [15] have achieved several MHz resolution [16], but likewise suffer from very low power levels above 2 THz [17]. Given the limitations of the sources described above, consideration of the use of free running TQCLs for spectroscopic applications in the 2-4 THz range is warranted.

Unlike mid-IR distributed feedback QCLs, which can be tuned several cm<sup>-1</sup> by, e.g., ramping the device bias voltage [18], a single longitudinal mode, fabry-perot-cavity TQCL provides only about 0.1 cm<sup>-1</sup> tuning range. To obtain a spectral bandwidth useful for spectroscopy we have mixed the TQCL radiation with a 2-20 GHz synthesized sweeper in a corner-cube-mounted Schottky diode and used primarily the upper sideband to measure several rotational transitions in low pressure D<sub>2</sub>O vapor. The spectroscopic results, in turn, enabled us to estimate the spectral content and center frequency of the TQCL source, when operating in either a pulsed or continuous wave (CW) mode.

## 2. Terahertz Quantum Cascade Laser Fabrication

The THz quantum cascade lasers were grown by the Photonics Center (University of Massachusetts Lowell) on semi-insulating (SI) GaAs substrates by a Veeco GenII Molecular Beam Epitaxy (MBE) system. The active region consisted of 80 periods of  $\text{Al}_{0.15}\text{Ga}_{0.85}\text{As}/\text{GaAs}$  superlattice based on the structure published by Barbieri *et al.* [19]. The thicknesses of every well and barrier were increased by approximately 10% compared to the original structure [20]. The active region was embedded between a 100-nm-thick top contact layer doped at  $5 \times 10^{18} \text{ cm}^{-3}$  and a 700-nm-thick bottom contact layer. The top contact metal, highly n+ doped bottom contact layer, and active region form a surface plasmon waveguide.

The epitaxial wafers were processed by Spire Corporation into 100 $\mu\text{m}$  ridge waveguide devices by first coating the wafers with photoresist, opening stripes, and depositing the front metal layers Au/Ge/Au/Ni/Au, followed by a resist liftoff process to remove the metal deposited on the resist-covered regions. The metallized stripes were then protected and reactive ion etching was used to define the ridges, whose adjacent material was removed to a depth extending into the 0.6- $\mu\text{m}$ -thick n-type conducting layer of GaAs. The protective resist was then removed, and a new layer of liftoff resist was applied. Following a second n-metal deposition, a second liftoff process was used to define the back metal contacts on both sides of the ridges. The wafers were then thinned to 140  $\mu\text{m}$  and back metal was applied to enable package soldering. The thinned wafers were then cleaved into die of various cavity lengths and die bonded into c-packages, after which wire bonds were made to the ridges (negative bias polarity) and to the striped contacts adjacent to both sides of the ridges (positive bias polarity).

## 3. THz QCL characterization

All of the fabricated lasers were tested and characterized in a pulsed and CW regime. Each TQCL was mounted on a cold surface of a liquid helium (LHe) dewar to maintain the laser temperature at about 10 K when it was not driven. The method of TQCL mounting is described in detail in Ref. [21]. Pulses of 1 ms duration with a repetition rate of 37 Hz were used to drive the TQCL in a pulsed regime. The spectra shown in Fig. 1 were obtained using a Fourier transform spectrometer (FTIR) (Bruker IFS 66v/s). A composite type Si-LHe-cooled bolometer was used as the detector. The frequencies of these lasers lie in a region from 2408 to 2496 GHz. Pulse and CW power levels between 1 and 3 mW were observed by using an absolute power meter [22].

The 2408 GHz laser was chosen for the remainder of this work. This laser had a 4 mm cavity length and a measured output power of about 1 mW. The threshold voltages and currents in CW and pulsed regimes were 3.4 V, 480 mA, and 3.1 V, 310 mA, respectively. The spectra at different bias voltages are shown in Figs. 1(a) and 1(b). The laser emitted radiation primarily in a single-longitudinal mode (SLM) up to 3.3 V in a pulsed mode, and 3.7 V in the CW mode. Other longitudinal modes if they existed were at the noise level, which was at least 20 dB down from the main mode.

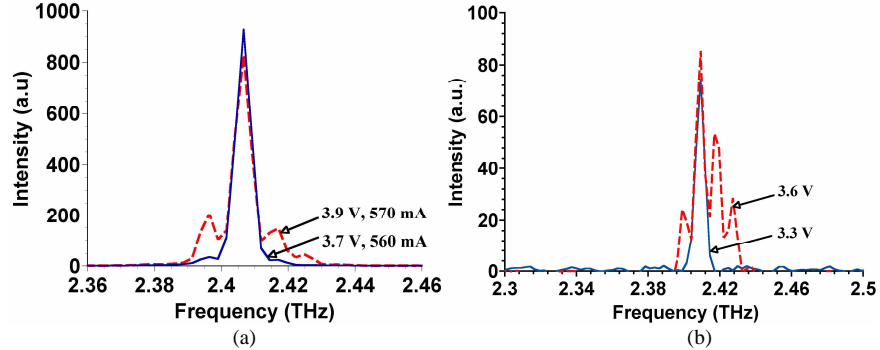


Fig. 1. Spectral intensity of the TQCL in CW (a) and pulsed (b) mode at different applied voltages.

#### 4. Sideband generation

A diagram of the sideband (SB) generation setup is shown in Fig. 2. The same TQCL dewar was used here. It was observed that the TQCL intensity was bistable when pulses with a rise time of 10 ns were applied. The laser stability increased significantly and the bistability was removed by using an RC low-pass filter, which increased the rise time of the pulses to 300  $\mu$ s. Neither temperature nor current stabilization of the TQCL was used in these experiments. A hollow dielectric Pyrex tube of 30 mm length and 1.5 mm inner diameter (ID) was used to significantly improve the laser radiation transverse mode content to a near-Gaussian beam profile [21].

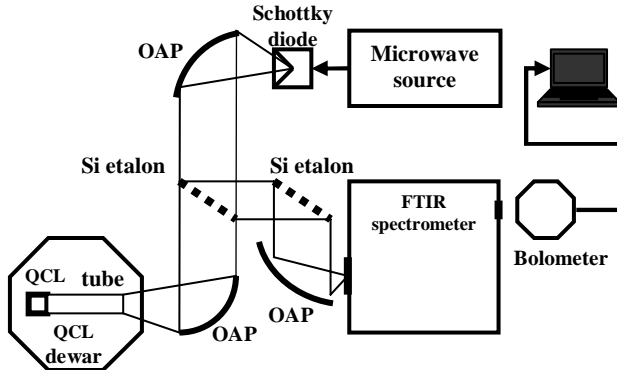


Fig. 2. Setup used for sideband generation experiment.

The TQCL radiation was collimated with an off-axis parabolic (OAP) mirror (focal length (FL) of 59.7 mm) and then focused with a second OAP (FL of 38.1 mm) onto the antenna of a whisker-contacted, corner-reflector-mounted Schottky barrier diode (SD) type 1T17, made by University of Virginia. The optimum SD position was determined by maximizing the SD video output signal. A maximum signal of 5.2 mV was achieved for 350  $\mu$ W of laser input power, giving a video responsivity of 15 V/W.

The SB radiation was generated by mixing the TQCL and microwave signals in the SD. The microwave signal was supplied by a 2-20 GHz synthesized sweeper (HP 83751B). 10dBm of microwave power was supplied to the diode through a coaxial cable into a bias tee. The THz SD output signal had several components with different frequencies: the sidebands of different orders, and the unshifted frequency laser signal with intensity comparable to or greater than that of the sidebands. Two high resistivity Si etalons with thicknesses of 1580

and  $1584 \mu\text{m}$  were used to separate the desired SB signal from the laser frequency component. The etalons were positioned at an angle of incidence of 42 degrees to transmit about 92% of the unshifted laser radiation and reflect about 80% of the first order sidebands when the synthesizer was set to 10 GHz. This provided about 20dB reduction in the twice-reflected intensity of the unshifted laser signal. To measure the SB power, the beam was focused with another OAP (FL=176 mm) onto the bolometer with a measured responsivity of  $2.08 \cdot 10^5 \text{ V/W}$ . When the TQCL emitted single longitudinal mode radiation (about  $240 \mu\text{W}$  of power), the measured SB power was approximately 150 nW, giving the power conversion efficiency of the SB generation system to be approximately  $6 \times 10^{-4}$ .

The spectra of the SB radiation with the TQCL operating in a single longitudinal mode were measured using the FTIR spectrometer at  $0.11 \text{ cm}^{-1}$  resolution. The spectrometer was set in the rapid scan mode with the TQCL operating CW and in step scan mode with the source pulsed. The same bolometer was used to acquire interferograms in both pulsed and CW modes. Fig. 3 shows composite spectra of the sideband radiation in the CW and pulsed modes.

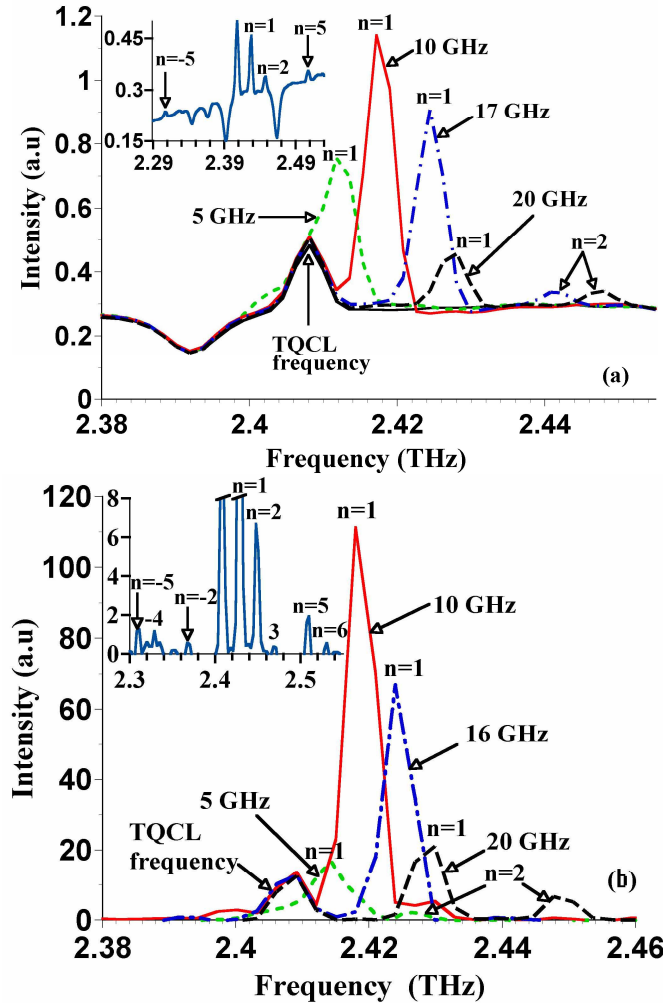


Fig. 3. Spectra of the sidebands produced by applying different microwave frequencies in CW (a) and pulsed (b) regimes with a 2.408 THz QCL. Insets are the sideband spectra corresponding to 20 GHz RF signal, which allow observing higher order sidebands.

The major difference between CW and pulsed spectra is the presence of a weak blackbody (BB) spectrum as a baseline in the CW case. In the case of rapid scan modulation, BB radiation from the room temperature, evacuated spectrometer box was directly modulated, together with the SB radiation, by the moving mirror, and is present in the CW spectra. In the step scan mode, the bolometer's output was fed to a lock-in amplifier, which was set to the frequency of the pulse generator that drove the TQCL. The lock-in output thus filtered out the unmodulated BB radiation. Absorption lines can be seen in the BB spectrum from the residual water vapor inside the vacuum box (Fig. 3(a)).

Absent from the spectra is the first order lower sideband (LSB), which was strongly absorbed along the 0.6 m atmospheric path length from the SD to the spectrometer by the strong water line at 2.39 THz. Si etalon reflection frequency dependence mainly explains the first order upper sideband intensities. Other harmonic sidebands, corresponding to 20 GHz microwave frequency, can be seen in the insets of Fig. 3.

### 5. Gas spectroscopy on D<sub>2</sub>O and THz QCL frequency measurements

The 3 GHz FTIR spectrometer resolution was inadequate for evaluating the SB spectral content, and thereby the TQCL bandwidth. The THz region is rich in rotational transitions in gases, and at low pressure the Doppler linewidth of these transitions lie in the range 2-10 MHz [23], which is comparable to the estimated longer-term frequency drift of the TQCL. Also, since the transition frequencies are often known to a very high precision, measurement of these lines with the SB radiation provides a precise value for the TQCL frequency. A review of tabulated terahertz spectral lines [24] revealed a number of strong rotational transitions in D<sub>2</sub>O that coincide with the SB spectra shown in Fig. 3.

To conduct the D<sub>2</sub>O gas spectroscopy experiments, the spectrometer was replaced with a 37-cm-long gas cell with plane-parallel non-wedged TPX input and output windows as shown in Fig. 4.

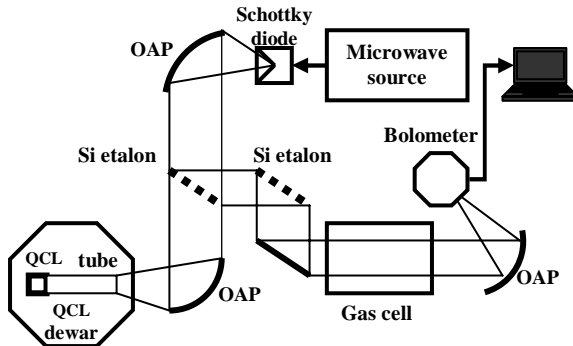


Fig. 4. Setup used for gas spectroscopy experiments.

SB radiation was directed through the cell and then focused onto the same bolometer with an OAP. The detected signal was measured with a lock-in amplifier and saved to a computer through a data acquisition card. The ratio of the SB power to the unshifted laser power was about 30. The maximum synthesizer sweep time of 100 s was used. Sampling at the preset number of 1600 points within a frequency range of 18 GHz (2-20 GHz) gave an incremental step of 11.25 MHz. Figure 5 displays the D<sub>2</sub>O spectra measured at a gas pressure of 500 mTorr as the microwave source was swept from 2 to 20 GHz. Figure 5(a) is the data obtained when the TQCL was operating CW, and Fig. 5(b) for pulsed operation at a 12.95% duty cycle (3.5 ms pulse length, 37 Hz). These plots are the ratio of sample and reference spectra

obtained with and without D<sub>2</sub>O in the cell. The SB intensity was low in the 6-7 GHz frequency range due to an impedance mismatch between the microwave source and the SD.

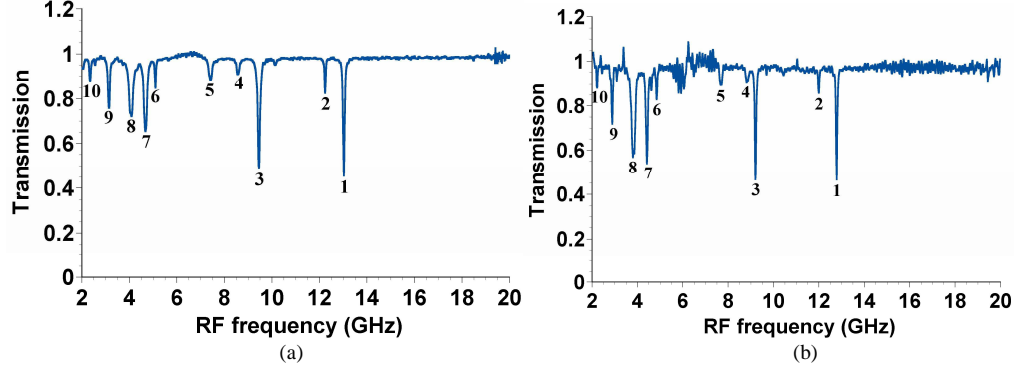


Fig. 5. Spectra of D<sub>2</sub>O at 500 mTorr in CW (a) mode and pulsed (b) mode produced by sweeping the microwave frequency from 2 to 20 GHz.

Four of the strongest lines (# 1, 3, 7, 9) were identified [24] as transitions at ( $\nu_{TQCL} + \nu_{microwave}$ ), i.e. the first harmonic, upper sideband and listed in Table 1 for a CW mode and Table 2 for a pulsed mode. The first line (2420782 MHz) was chosen as a reference line. All frequencies are rounded to the nearest MHz.  $\Delta\nu$  is the difference between obtained and tabulated frequencies of transitions. Intensity is a base 10 logarithm of the integrated intensity. The quantum numbers correspond to the upper and lower rotational states of the transitions.

Table 1. List of 4 strongest pure rotational transitions of D<sub>2</sub>O for CW mode.

Line	SB	RFfreq. (MHz)	Obtained freq.(MHz)	Tabulated freq.[24].	Molecule	$\Delta\nu$	Intensity	$J'K'_aK'_b$	$J''K''_aK''_b$
9	1USB	3146	2410897	2410889	D <sub>2</sub> O	8	-1.1626	5 5 0	5 4 1
7	1USB	4680	2412431	2412422	D <sub>2</sub> O	9	-0.8611	5 5 1	5 4 2
3	1USB	9454	2417205	2417205	D <sub>2</sub> O	0	-1.1819	9 1 8	9 0 9
1	1USB	13031	2420782	2420782	D <sub>2</sub> O	0	-1.4903	10 5 6	10 4 7

Table 2. List of 4 strongest pure rotational transitions of D<sub>2</sub>O for pulsed mode.

Line	SB	RFfreq. (MHz)	Obtained freq.(MHz)	Tabulated freq.[24].	Molecule	$\Delta\nu$	Intensity	$J'K'_aK'_b$	$J''K''_aK''_b$
9	1USB	2895	2410893	2410889	D <sub>2</sub> O	4	-1.1626	5 5 0	5 4 1
7	1USB	4425	2412423	2412422	D <sub>2</sub> O	1	-0.8611	5 5 1	5 4 2
3	1USB	9208	2417206	2417205	D <sub>2</sub> O	1	-1.1819	9 1 8	9 0 9
1	1USB	12784	2420782	2420782	D <sub>2</sub> O	0	-1.4903	10 5 6	10 4 7

The remaining transitions have not yet been unambiguously identified. These transitions in the CW mode were shifted up about 250 MHz in microwave frequency, compared to the corresponding pulse mode data, as a result of the red shift of the TQCL with increasing temperature. Two lines (4, 5) were shifted down 250 MHz because they were produced by the first harmonic lower sideband. Changing a QCL frequency also allows identifying the order of the harmonics. If the laser shift is  $\Delta f$  then the microwave frequency shift in any observed transition is  $\Delta f' = \pm \Delta f / n$ , where  $n$  is the order of the harmonic and (+, -) refers to the (upper, lower) sideband. This allowed identifying line 10 as the line produced by the second harmonic upper sideband since  $\Delta f' = 125\text{MHz}$ .

From previous measurements of  $(1/\nu)(d\nu/dT)$  and the frequency shift of 250 MHz we estimated that the CW operating temperature of the TQCL was 1.6 K higher than that in the pulsed mode based on the temperature tunability obtained from Ref. [7] and 2.5 K based on the results from Ref. [5]. This temperature difference is so small because of the pulse structure with a very long rise time. It is worth noting that the difference in cold plate temperature, measured by a temperature sensor mounted on the plate, was about 15 K (13 K vs 28 K). Comparison of  $\Delta\nu$  for the transitions in CW versus pulsed demonstrates that the same precision can be achieved in either case once the data is referenced to a known transition. The relatively large frequency step (11.25 MHz) used in the 2-20 GHz synthesizer sweep was the limiting factor in determining the precision of the transition frequencies. The operating frequencies of the TQCL in the CW and pulsed regime (at a 12.95% duty cycle) can be determined to the precision of these measurements, approximately 10 MHz. The results are 2407750 MHz (CW) and 2408000 MHz (pulsed).

## 6. Gas spectroscopy on D<sub>2</sub>O and THz QCL linewidth measurements

To examine the laser linewidth and drift at higher resolution we made a series of SB sweeps over the J=10, K<sub>a</sub>=4, K<sub>b</sub>=7 to J=10, K<sub>a</sub>=5, K<sub>b</sub>=6 transition at different D<sub>2</sub>O gas pressures. The synthesizer was swept over about 400 MHz and sampled at 1600 points providing an incremental step of approximately 250 kHz. Figures 6(a) and 6(b) are plots of the relative transmitted intensity through the gas cell for the CW and pulsed cases.

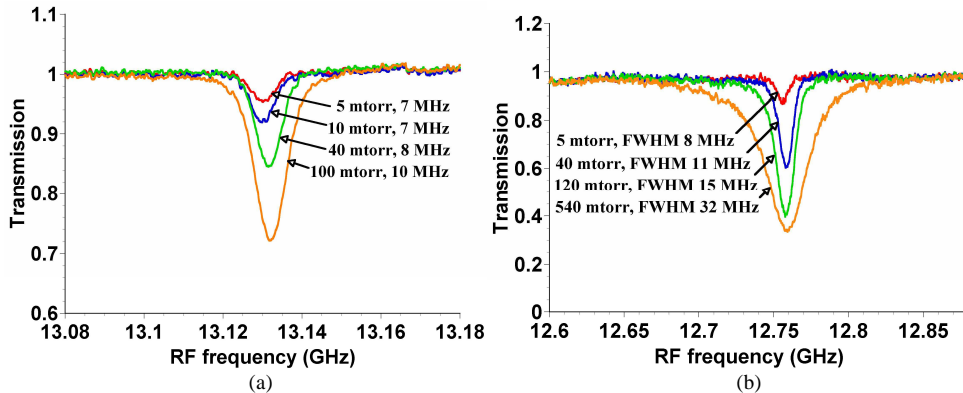


Fig. 6. Spectra of 2420782 MHz line of D<sub>2</sub>O in CW (a) mode and pulsed (b) mode at different pressures of D<sub>2</sub>O.

The D<sub>2</sub>O spectra of the line #1 ( $\nu=2420782$  MHz) were measured for gas pressures from 3 torr down to several millitorr. Since the errors in the linewidth measurements were about 250 kHz, the linewidths were rounded to the nearest MHz. The theoretical Doppler linewidth of line #1 is  $\Delta\nu = 6.7$  MHz. The measured linewidth of line #1 continued to narrow down to approximately the theoretical Doppler linewidth. A value of 7 MHz was measured in the CW

mode and, somewhat surprisingly, 8 MHz in the pulsed mode where a frequency chirp might be anticipated.

The measured spectra are the convolutions of the D<sub>2</sub>O Gaussian molecular lineshape of a width  $\Delta\nu_{D_2O}$  with the TQCL spectral lineshape of a width  $\Delta\nu_{TQCL}$ . The laser lineshape over a long period of time (seconds) can be assumed for simplicity to be a Gaussian instead of the actual shape, which is close to a rectangular one [4] (this simplification would only widen the estimated TQCL spectral content). The linewidth of convolved Gaussian spectra is given by the formula  $\Delta\nu = \sqrt{\Delta\nu_{D_2O}^2 + \Delta\nu_{TQCL}^2}$ . It gives the laser linewidth,  $\Delta\nu_{TQCL}$ , of about 2 MHz (CW mode) and 4.4 MHz (pulsed mode) for the case of the lowest pressures, where the time to sweep across the width of the line was about 2 s. The frequency drift and the laser linewidth over a longer period of time can be deduced from the centerline drift of absorption lines in Fig. 6 and were observed to be less than 3 MHz. The time intervals between measurements were about 5-10 minutes. Thus the long-term (over minutes) linewidth of the TQCL does not exceed 4.4 MHz.

The observed narrow linewidth in the pulsed mode can be understood from the current profile through the TQCL given in Fig. 7. Since the pulse widths were 3.5 ms with a time,  $\Delta t_{AB}=300\text{ }\mu\text{s}$ , to reach the threshold current (between points A and B), we can assume that the TQCL reached a temperature very close to an equilibrium one during  $\Delta t_{AB}$  before it started lasing at the threshold level. This would significantly reduce the temperature change and as a consequence the chirp bandwidth during the lasing time. Based on the frequency-vs-current tuning of 6 GHz/A measured by Barbieri [5] for a similar device, the current pulse must be within 0.8 mA of its maximum value of 383 mA (3.3 V) for the TQCL to be within its spectroscopically-determined 4.4 MHz linewidth. Therefore, any initial chirp effect greater than 4.4 MHz would be completed during a time interval,  $\Delta t_{\text{chirp}} \sim 500\text{ }\mu\text{s}$ , after threshold was reached but before the TQCL current reached 382.2 mA (between points B and C). Since  $\Delta t_{\text{chirp}} < \Delta t_{CD}$ , the time between points C and D, the chirp contribution to the pulse spectra is no greater than the ratio 0.5ms/2.8ms. The slow bolometric detector response time ( $\tau \sim 1\text{ ms}$ ) will further decrease the chirp contribution to at least an order of magnitude below the “steady state” contribution. Evidence of a residual chirp can be seen in the spectral lineshape measured at the highest pressure in Fig. 6(b), where a slight broadening on the low frequency side is evident. For this sufficiently wide linewidth the integrated effect of the chirp exceeds the system noise. The chirp at the end of the pulse will negligibly affect the linewidth since it lasts for only about 8  $\mu\text{s}$  (points D and E). At lower pressures where the line broadening is reduced and the lineshape transitions from a Voigt to a Gaussian profile the chirp contribution is undetectable. Since the maximum and the threshold currents were 383 mA (3.3 V) and 345 mA (3.1 V), respectively, a chirp magnitude of about 230 MHz was estimated from Barbieri’s value for dv/dI.

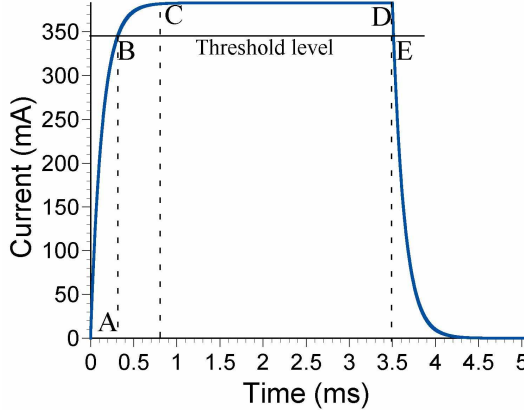


Fig. 7. TQCL current in the pulsed mode as a function of time.

To completely eliminate the chirp a fast detector ( $\tau \leq 1 \mu\text{s}$ ) could be used along with electronics to sample the signal only on the postchirp portion of the pulse,  $\Delta t_{CD}$ . This quasi-CW mode of operation would offer a considerable reduction in liquid helium consumption without sacrificing resolution of the tunable SB radiation, since the boil-off rate is inversely proportional to the duty cycle.

## 7. Conclusion

The first sideband generator based on mixing a THz QCL with a microwave signal in a corner cube Schottky diode has been reported in this paper. The tunable source was tested by using it in rotational spectroscopy on  $\text{D}_2\text{O}$ . The TQCL long-term linewidths of 2 MHz (CW regime) and 4.4 MHz (pulsed regime) were found. A quasi-CW mode proposed in this paper would result in a significant reduction of liquid He consumption in comparison with CW operation. Sideband frequency tunability provides the possibility of stabilizing the THz QCL frequency by locking it to the center of a gas absorption line.

## Acknowledgments

We are grateful to E. Ehasz for providing the gas cell for this experiment. This work was supported by the U.S. Army National Ground Intelligence Center and the Department of Homeland Security.